

# Line-profile variation in $\tau$ Herculis

Seiji Masuda and Ryuko Hirata

Department of Astronomy, Faculty of Science, Kyoto University, Sakyo-ku, Kyoto 606-8502, Japan  
(masuda@kusastro.kyoto-u.ac.jp; hirata@kusastro.kyoto-u.ac.jp)

Received 23 December 1998 / Accepted 31 January 2000

**Abstract.** Based on a time series of high-resolution spectra at He I  $\lambda 4471$  and Mg II  $\lambda 4481$ , we have detected the line-profile variation of  $\tau$  Her, one of the newly discovered Slowly Pulsating B Stars by Hipparcos.

A period analysis has been performed for the radial velocities of Mg II  $\lambda 4481$ . A best estimated period of 1.17 d or its one-day alias 0.536 d is different from its photometric period (1.25 d) derived from the Hipparcos mission.

**Key words:** line: profiles – stars: early-type – stars: oscillations – stars: variables: general – stars: individual:  $\tau$  Her

## 1. Introduction

Slowly Pulsating B Stars (hereafter SPBs) have been discovered in the course of a systematic observational program of a homogeneous sample of stars, using the Geneva photometry (Waelkens 1991, and references therein). They are main-sequence mid-B-type variable stars with periods of the order of one day. Observational characteristics of this group have been summarized by North & Paltani (1994).

Waelkens (1991) interpreted the photometric behaviors of SPBs in terms of non-radial pulsation in the  $g$ -modes with large radial wavenumber  $k$  and low order  $l$ . The pulsation mechanism of SPBs has been attributed to the  $\kappa$ -mechanism, acting in the metal opacity bump at  $T \sim 2 \times 10^5$  K calculated with the new OPAL (Iglesias et al. 1992) and OP (Seaton et al. 1994) opacity data (Gautschy & Saio 1993; Dziembowski et al. 1993). Moskalik (1995) gave a review on theoretical instability domains in the HR diagram for B-type pulsators:  $\beta$  Cep stars and SPBs. From a stellar seismological point of view, SPBs are fruitful targets for understanding the internal structure of massive stars because  $g$ -modes penetrate the whole radiative interior of a star.

Waelkens et al. (1998) have recently discovered 72 new SPBs based on the Hipparcos photometry. These new SPBs rather well cover the theoretical instability domain, and are diversely distributed with respect to the period and the rotational velocity. Thus, it is a good unbiased sample for the study of B-type pulsating stars.

Most SPBs have so far been investigated photometrically. Since the higher-order modes ( $l \geq 3$ ) are hardly detected with

photometry, it is important to observe these new SPBs spectroscopically for understanding the overall pulsating nature of this group. However, spectroscopic studies have been carried out only for a limited number of SPBs (North & Paltani 1994; Aerts et al. 1999).

$\tau$  Her (HR 6092 = HD 147394 = HIP 79992,  $m_V = 3.9$ ) is one of the new SPBs found by the Hipparcos mission, with a period of  $1.24970 \pm 0.00008$  d (ESA 1997). This star is a B5IV standard star of the MK spectral classification (Morgan & Keenan 1973), with the rotational velocity of  $30 \text{ km s}^{-1}$  (Slettebak et al. 1975). Wolff (1978) reported that the radial velocity of  $\tau$  Her is variable and suggested that it is a single-line spectroscopic binary with a period of 4.95 d. Abt & Levy (1978) also studied the radial velocity of  $\tau$  Her, covering the epochs including but longer than that of Wolff (1978), and concluded its constancy. No line-profile variation in  $\tau$  Her has been reported so far.

## 2. Observations and data reduction

The observations were carried out in August 5 – 10, 1998 at the Okayama Astrophysical Observatory (a branch of the National Astronomical Observatory, an inter-university research institute operated by the Ministry of Education, Science, Sports and Culture of Japan), using the 1.88m telescope with the coude spectrograph equipped with a  $1800 \text{ grooves mm}^{-1}$  grating, which gives dispersion of  $\sim 5.5 \text{ \AA mm}^{-1}$ . We used a RCA SID503EX CCD (pixel size is  $15 \mu\text{m} \times 15 \mu\text{m}$ ;  $1024 \times 640$  pixels) as a detector, and set a slit width to  $120 \mu\text{m}$  which corresponds to  $0.45 \text{ arcsec}$  projected on the sky and to 2 pixels on the CCD. The spectral resolution was confirmed to be 27 000 from the typical FWHM (2.0 pixels) of comparison lines. Rather bad weather condition permitted us to obtain only 30 spectra in five nights for He I  $\lambda 4471$  and Mg II  $\lambda 4481$ . The exposure time was between 5 to 30 minutes, depending on sky condition.

We reduced the data, using the IRAF<sup>1</sup> software package. After the standard reductions for CCD (bias-subtraction, flat-fielding, spectral extraction, and wavelength calibration), all spectra were reduced to the heliocentric frame and normalized

---

<sup>1</sup> IRAF is distributed by the National Optical Astronomy Observatories, which is operated by the Association of Universities for Research in Astronomy, Inc. under cooperative agreement with the National Science Foundation.

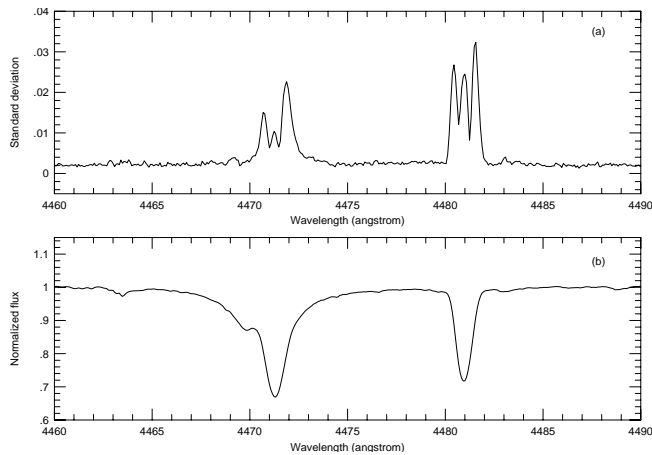


**Fig. 1a and b.** **a** Standard deviation and **b** mean profile of all 30 spectra in the region of He I  $\lambda$ 4471 and Mg II  $\lambda$ 4481

to the local continuum. The signal to noise ratios were 240 – 410 at the continuum level. The journal of the observations is summarized in Table 1.

### 3. Results

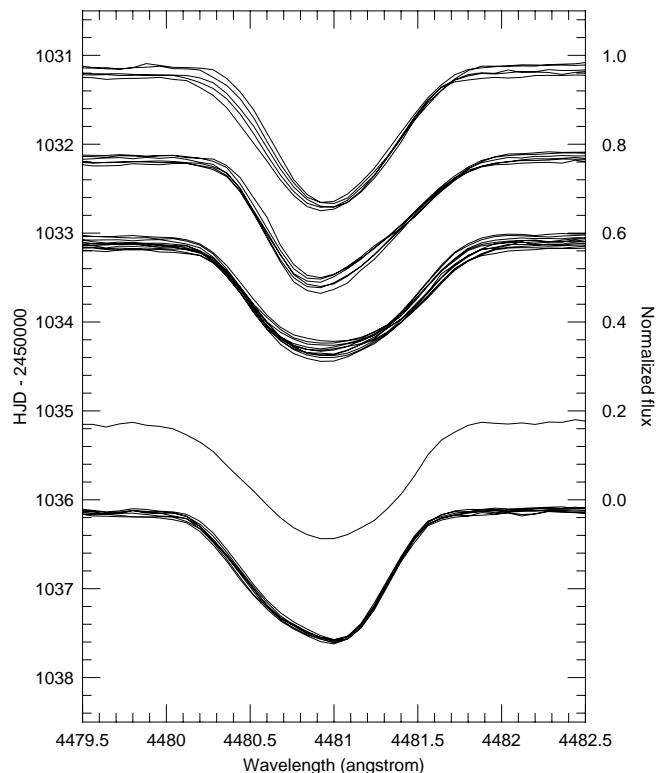
#### 3.1. Line-profile variation

Fig. 1a shows the standard deviation for all 30 spectra at each wavelength point, together with the mean profile (Fig. 1b). The deviations in absorption lines (He I  $\lambda$ 4471 and Mg II  $\lambda$ 4481) are much larger than those at the continuum. This demonstrates the existence of line-profile variation in  $\tau$  Her. Since forbidden He I  $\lambda$ 4469.9 contaminates He I  $\lambda$ 4471, we focused on the analysis of Mg II  $\lambda$ 4481.

In Fig. 2 we show a time series of the profile of Mg II  $\lambda$ 4481. Spectra are offset proportionally to their data acquisition (mid-exposure) time, expressed in heliocentric Julian day (HJD). The variation of the line-profile in this line is clearly seen in the line depth and asymmetry. The line was deep and slightly asymmetric in the first night (HJD 2 451 031). It changed to a red-winged profile with a blue-shifted core in the second night. The line-profiles in the third night were rather symmetric and shallow, and in the next night, being still shallow but slightly asymmetric. In the last night, the line became deeper with the blue-winged profile and it looks like a mirror image of the profile in the second night.

#### 3.2. Radial velocity and equivalent width variations

We examined the radial velocity and equivalent width of Mg II  $\lambda$ 4481. The radial velocity was estimated from the first moment of the line-profile (i.e., depth-weighted radial velocity) for the rest wavelength of 4481.228 Å. We also calculated the second and third moments (see Eqs. (2) and (3) of North & Paltani (1994) for the definition), after correcting the  $\gamma$  velocity ( $-17.3 \text{ km s}^{-1}$ ). These quantities are listed in Table 1. In Fig. 3, we show the time variation of the radial velocity (Fig. 3a) and the equivalent width (Fig. 3b).



**Fig. 2.** Time series of the profiles of Mg II  $\lambda$ 4481. The vertical offset is proportional to the data acquisition time (HJD), which increases downwards

We performed a period analysis of the radial velocity with the CLEAN algorithm (Roberts et al. 1987), although the total number of frames is small and the result would be strongly influenced by one-day alias. The resulting periodogram is shown in Fig. 4a, together with the window function (Fig. 4b). We examined the frequencies corresponding to the highest six peaks ( $f_1 = 0.145$ ,  $f_2 = 0.858$ ,  $f_3 = 1.147$ ,  $f_4 = 1.865$ ,  $f_5 = 2.094$ , and  $f_6 = 2.868 \text{ c d}^{-1}$ ) in Fig. 4a as the trial frequency, and derived each CLEANed spectrum. In Fig. 4c, we show CLEANed spectra for  $f_2$  and  $f_4$ , whose peaks have almost the same height. The respective powers of CLEANed spectrum peak for other four frequencies are smaller than those for  $f_2$  and  $f_4$ . Moreover, the pseudo peaks of wavy pattern are more prominent for these four frequencies. We conclude that the most probable frequency is  $f_2$  ( $P = 1.17 \text{ d}$ ) or its one-day alias  $f_4 = 1 + f_2$  ( $P = 0.536 \text{ d}$ ). The residual frequencies are the aliases connected by  $f_1 = 1 - f_2$ ,  $f_3 = 2 - f_2$ ,  $f_5 = 3 - f_2$ , and  $f_6 = 2 + f_2$ . Fig. 5 shows the radial velocity curves folded by these two periods. The error of period analysis was roughly estimated from the inspection of the folded velocity curves stepped by 0.01 d around  $P = 1.17 \text{ d}$  and by 0.001 d around  $P = 0.536 \text{ d}$ . It is 0.05 d for the former and 0.005 d for the latter.

A period analysis of the equivalent width yields no meaningful period. Its total variation is only 15 mÅ, which implies that it is rather constant within the accuracy of our measurements. We also examined the second and third moments of the

**Table 1.** Journal of observations and derived quantities ( $t_{\text{exp}}$ : exposure time, EW: equivalent width, RV: radial velocity,  $m_2$  and  $m_3$ : the second and third moments of the profile)

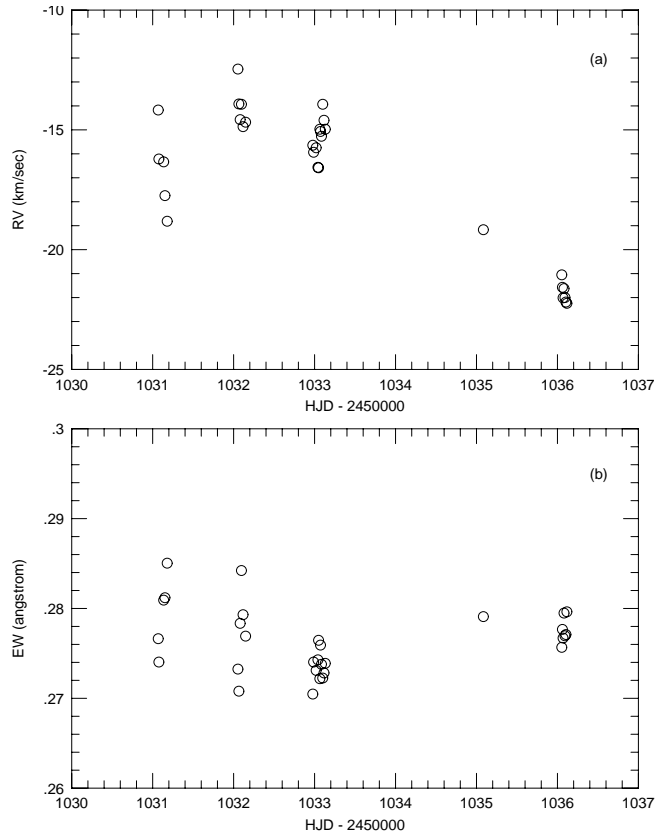
HJD -2450000	$t_{\text{exp}}$ [s]	S/N	EW [Å]	RV [km s <sup>-1</sup> ]	$m_2$	$m_3$
1031.067	600	270	0.2767	-14.17	0.1153	0.01685
1031.078	900	320	0.2741	-16.22	0.1144	0.00699
1031.136	900	270	0.2809	-16.34	0.1185	0.00497
1031.150	1200	290	0.2812	-17.74	0.1195	-0.00167
1031.180	1800	260	0.2850	-18.81	0.1241	-0.00567
1032.053	600	320	0.2732	-12.46	0.1406	0.03341
1032.066	900	380	0.2708	-13.92	0.1343	0.02622
1032.079	900	320	0.2783	-14.57	0.1384	0.02371
1032.098	1200	240	0.2842	-13.93	0.1409	0.02607
1032.117	1800	290	0.2793	-14.87	0.1356	0.02068
1032.149	1800	280	0.2769	-14.68	0.1269	0.02080
1032.976	600	340	0.2705	-15.65	0.1445	0.01050
1032.988	900	330	0.2740	-15.94	0.1461	0.01000
1033.019	720	360	0.2731	-15.75	0.1479	0.01168
1033.041	300	280	0.2743	-16.56	0.1479	0.00787
1033.050	600	320	0.2765	-16.58	0.1488	0.00829
1033.065	600	340	0.2722	-14.97	0.1482	0.01777
1033.074	600	240	0.2759	-15.07	0.1481	0.01719
1033.085	900	280	0.2738	-15.27	0.1482	0.01672
1033.102	1200	410	0.2723	-13.93	0.1500	0.02465
1033.117	1200	340	0.2728	-14.60	0.1486	0.02027
1033.133	1200	310	0.2739	-14.97	0.1465	0.01903
1035.086	1200	250	0.2791	-19.16	0.1430	-0.01419
1036.053	600	410	0.2757	-21.06	0.1206	-0.01912
1036.062	600	370	0.2777	-21.57	0.1230	-0.02146
1036.071	600	360	0.2767	-22.02	0.1235	-0.02301
1036.081	600	310	0.2795	-21.63	0.1251	-0.02265
1036.093	900	360	0.2770	-22.00	0.1244	-0.02399
1036.106	900	320	0.2771	-22.18	0.1249	-0.02481
1036.118	900	270	0.2796	-22.24	0.1275	-0.02569

line-profile, and confirmed that they vary with almost the same period as in the first moment.

#### 4. Discussion

The period derived from our present spectroscopic study of  $\tau$  Her ( $P = 1.17 \pm 0.05$  d or  $P = 0.536 \pm 0.005$  d) is different from the photometric one ( $P = 1.25$  d) from the Hipparcos satellite (ESA 1997). Although the photometric period is only slightly beyond our error limit in the case of 1.17 d period, we can conclude that these two periods differ from each other for the following reasons. When we adopt the 1.25 d period, our data obtained in the first and last nights cover almost the same phase. However, the radial velocities in these two nights are clearly different (see Fig. 3a). Furthermore, the line asymmetry is also different in these two nights (see Fig. 2).

The period difference is expected when  $\tau$  Her is multiperiodic. Aerts et al. (1999) reported that the periods derived from their spectroscopic data, the Hipparcos and their ground-based Geneva photometry differ with each other in HD 215573, though they are almost the same for most of their observed SPBs.

**Fig. 3a and b.** Time variation of **a** the radial velocity and **b** the equivalent width of Mg II  $\lambda 4481$ 

Although we estimated the radial velocities using not the line core but the first moment of the overall line-profile as a more accurate measure, the derived velocities are consistent with the past results regarding the systemic  $\gamma$  velocity;  $-17.3$  km s<sup>-1</sup> (this work),  $-17.2$  km s<sup>-1</sup> (Abt & Levy 1978), and  $-13.8$  km s<sup>-1</sup> (Wilson 1953), and to the range of velocity variation;  $-22.2$  –  $-12.5$  km s<sup>-1</sup> (this work),  $-21.6$  –  $-11.2$  km s<sup>-1</sup> (Wolff 1978), and  $-22.2$  –  $-9.9$  km s<sup>-1</sup> (Abt & Levy 1978). The 4.95 d periodicity reported by Wolff (1978) was not detected from our data.

Waelkens et al. (1998) gave a preliminary estimate of the effective temperature ( $\log T_{\text{eff}} = 4.18$ ) and the luminosity ( $\log L/L_{\odot} = 3.33$ ) for  $\tau$  Her, by using the data of the Geneva photometry. Its position on the theoretical HR diagram is near the boundary of theoretically predicted instability strip of SPBs with metallicity  $Z = 0.02$ . We can guess the pulsation mode using Fig. 8 of Dziembowski et al. (1993) from the effective temperature and period. In the case of the period of 1.17 d, the line-profile variation in  $\tau$  Her could be interpreted in terms of the high-order  $g$ -mode non-radial pulsation with  $l = 2$  for a  $5M_{\odot}$  star, though we cannot exclude the possibility of  $l = 1$  in the case of a lower mass star. If the period is 0.536 d, the  $l = 2$  mode is highly probable.

More extensive data are required in order to determine its periods accurately and to derive the modes of non-radial pulsation. We are planning to perform a multi-line monitoring of  $\tau$  Her

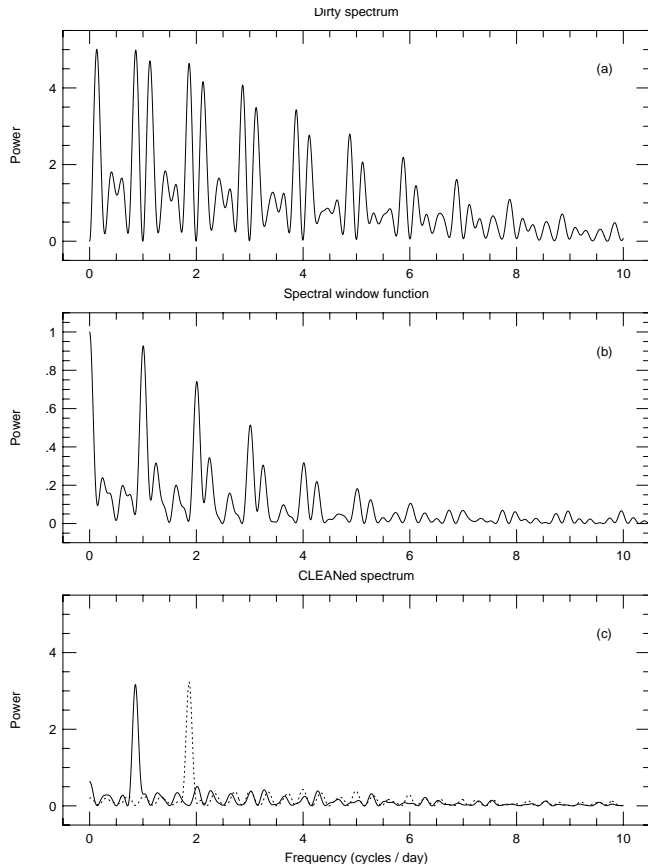


**Fig. 4a – c.** Time series analysis of the radial velocity variation of Mg II  $\lambda$ 4481; **a** dirty spectrum, **b** spectral window function, **c** CLEANed spectrum for the trial frequency of 0.858 (continuous) and 1.865 (dash)  $\text{c d}^{-1}$  after ten iterations with gain  $g = 0.5$

in the next season with HIDES (HIGH Dispersion Echelle Spectrograph) at the Okayama Astrophysical Observatory, which is now under development.

*Acknowledgements.* The authors are grateful to the staff members of the Okayama Astrophysical Observatory for their support during our observational run. Thanks are also due to H. Iwamatsu, T. Kawano, and T. Matsumoto for their help in our observations. SM would like to acknowledge M. Kato for providing him with the CLEAN code. We would also thank the referee, Dr. P. North, for his constructive suggestions, by which the manuscript was much improved. This research has made use of the Simbad database, operated at CDS, Strasbourg, France, and NASA's Astrophysics Data System Abstract Service.

## References

- Abt H.A., Levy S.G., 1978, *ApJS* 36, 241  
 Aerts C., De Cat P., Peeters E., et al., 1999, *A&A* 343, 872  
 Dziembowski W.A., Moskalik P., Pamyatnykh A.A., 1993, *MNRAS* 265, 588

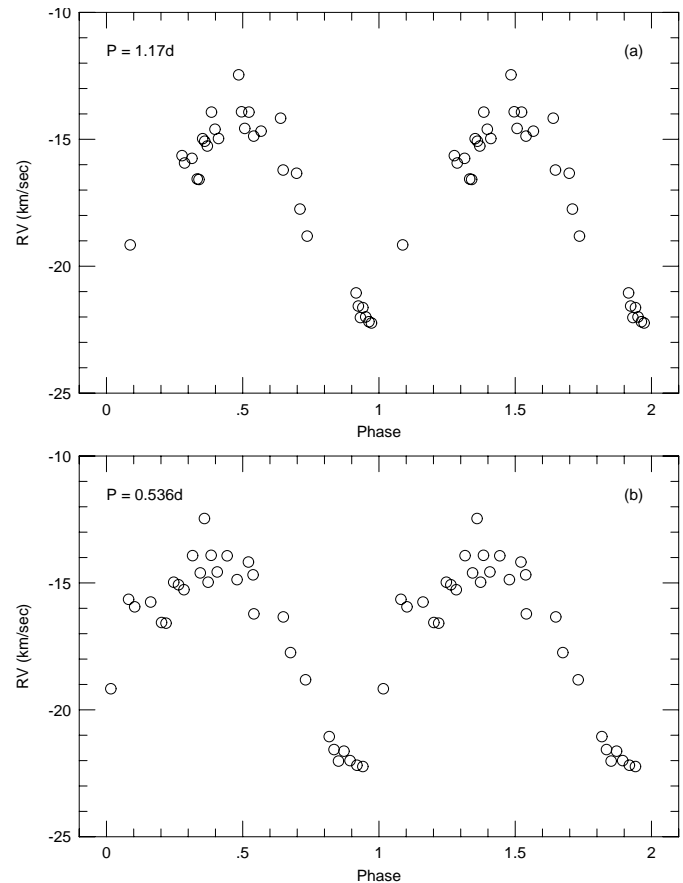


**Fig. 5a and b.** Radial velocity curves of Mg II  $\lambda$ 4481; **a** folded by  $P = 1.17$  d, **b** folded by  $P = 0.536$  d

- ESA, 1997, The Hipparcos and Tycho Catalogues. ESA SP-1200  
 Gautschy A., Saio H., 1993, *MNRAS* 262, 213  
 Iglesias C.A., Rogers F.J., Wilson B.G., 1992, *ApJ* 397, 717  
 Morgan W.W., Keenan P.C., 1973, *ARA&A* 11, 29  
 Moskalik P., 1995, In: Stobie R.S., Whitelock P.A. (eds.) *Astrophysical Applications of Stellar Pulsation*. ASP Conference Series Vol. 83, p. 44  
 North P., Paltani S., 1994, *A&A* 288, 155  
 Roberts D.H., Lehár J., Dreher J.W., 1987, *AJ* 93, 968  
 Seaton M.J., Yan Y., Mihalas D., Pradhan A.K., 1994, *MNRAS* 266, 805  
 Slettebak A., Collins G.W. II, Boyce P.B., White N.M., Parkinson T.D., 1975, *ApJS* 29, 137  
 Waelkens C., 1991, *A&A* 246, 453  
 Waelkens C., Aerts C., Kestens E., Grenon M., Eyer L., 1998, *A&A* 330, 215  
 Wilson R.E., 1953, *General Catalogue of Stellar Radial Velocities*. Carnegie Institution of Washington  
 Wolff S.C., 1978, *ApJ* 222, 556